(Received 10 February 2024, Accepted 11 June 2024, Scheduled 24 June 2024)

Dispersion Compensation for Spoof Plasmonic Circuits

Wenyao Zou[1,2], Wenxuan Tang[1,2], Jingjing Zhang[1,2,*], Shanwen Luo[1,2], Facheng Liu[1,2], Hao Chi Zhang[1,2], Yu Luo[3], and Tie Jun Cui[1,2,*]

[1]*Institute of Electromagnetic Space, Southeast University, Nanjing 210096, China*
[2]*State Key Laboratory of Millimeter Waves, Southeast University, Nanjing 210096, China*
[3]*Key Laboratory of Radar Imaging and Microwave Photonics Nanjing University of Aeronautics and Astronautics, Nanjing 211106, China*

ABSTRACT: Spoof surface plasmon polariton (SSPP) transmission lines (TLs) provide a possible way to confining transmitted signals in deep subwavelength scale. SSPP TLs can suppress the mutual coupling between adjacent channels and improve the signal integrity, providing a promising alternative to conventional transmission lines. However, SSPP structures generally possess strong chromatic dispersion (i.e., signals at different frequencies propagate with different velocities), resulting in significant pulse distortion. Such drawback greatly hampers the practical application of SSPP TLs, especially in the long range transmission. To tackle this bottleneck problem, we propose a dispersion-compensation mechanism, where a section of judiciously designed TL with an opposite-dispersion characteristic is added to the SSPP circuit to achieve minimized total dispersion of the link within a broad frequency range. The experimental results indicate an impressive improvement of 72.46% for the SSPP transmission line in the stability of the circuit group delay after applying the dispersion compensation approach. This hybrid transmission line has high transmission efficiency without inducing group delay dispersion of the signals. Our design scheme can be easily extended to other frequency band, offering a possible solution to high-performance signal transmission in future integrated circuits.

1. INTRODUCTION

Microstrip lines are widely used in various circuits; however, in dense circuits with multiple layers and a great number of parallel lines, the current flow in the circuit tends to crowd towards the surface of metal due to the proximity effect, leading to high ohmic loss as well as large electromagnetic (EM) coupling [1–3]. This is one of the challenges facing the development of high-frequency transmission and circuit integration.

Surface plasmon polaritons (SPPs), a special kind of surface electromagnetic (EM) waves are supported by collective oscillations of the delocalized electrons between metal and dielectric materials, and can confine EM waves on a subwavelength scale with high intensity [4–7]. The discovery of SPP opens up a previously inaccessible length scale for the optical research, implying the possibility for the miniature photonic circuits and interconnects [8–14]. In addition, the surface plasma's subwave length characteristics allow the electromagnetic field near the metal or electrical medium interface to be strongly localized and enhanced, with excellent transmission properties such as high bonding, short working wavelengths, high intervals, and therefore widely used in the fields of photodetection [15, 16] photonics [17–19], imaging [20–24], sensing, etc. [19, 23, 25, 26]. Thus, compared to traditional transmission lines, the SSPP transmission line has the characteristics of small crosstalk, enabling efficient transmission in the microwave and terahertz frequency bands [27–32]. On the other hand, the convenience of processing, low cost, and ultrathinness also provide the possibility for the wide application of SSPP transmission lines in the field of integrated circuits [33–35].

SSPP has special dispersion characteristics which can be engineered by judiciously designing the structures [36]. This special property has attracted a lot of studies, allowing a number of different devices with novel functionalities, such as multi-band helicity-controlled directional SSPP coupling and [37] achromatic devices based on SSPPs dispersion characteristics [38, 39]. However, the dispersion effect is also one of the greatest issues in the SSPP transmission which lead to signal distortion and limit the maximum transmission length and/or speed. As a consequence of dispersion, pulse broadening occurs, leading to an overlap of the neighbored symbols in cases of high data rates. Strong dispersion will make it difficult to distinguish the adjacent pulses at the recipient of the signal. Even for moderate broadening, the inter-symbol interference can still cause the degradation of detected signals. Therefore, tackling the issue induced by the dispersion is crucial to the promotion of SSPP transmission lines in communication systems [40–44]. However, despite its importance, this problem has not been solved so far to the best of our knowledge.

In fiber optic systems, dispersion compensation fiber technology is widely used, i.e., in conventional fiber, adding negative dispersion fiber compensation to ensure that the total color dispersion of the entire fiber line is approximately zero, thus achieving high speed, large capacity, and long distance communication. Inspired by this idea, we have proposed a tech-

* Corresponding authors: Jingjing Zhang (zhangjingjing@seu.edu.cn); Tie Jun Cui (tjcui@seu.edu.cn).

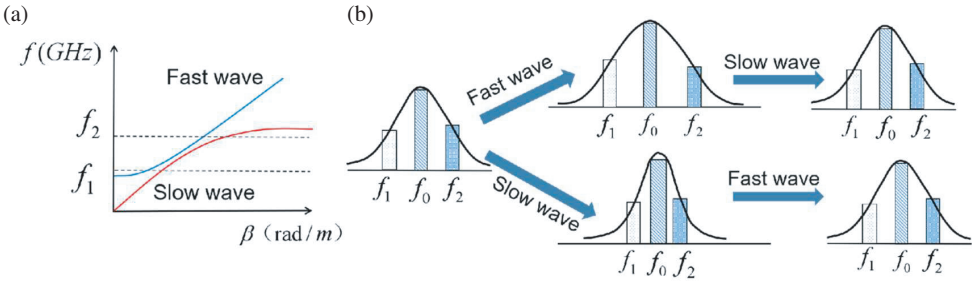

FIGURE 1. Conceptual basis of signal distortion compensation. The dispersion properties of various transmission lines can be employed to compensate for signal distortion. (a) Transmission lines with a slow wave property and a fast wave property show different dispersion characteristics. The slope of the dispersion curve determines the transmission speed of signals at certain frequencies. (b) The complete process of signal transmission compensation in the fast wave transmission line and the slow wave transmission line.

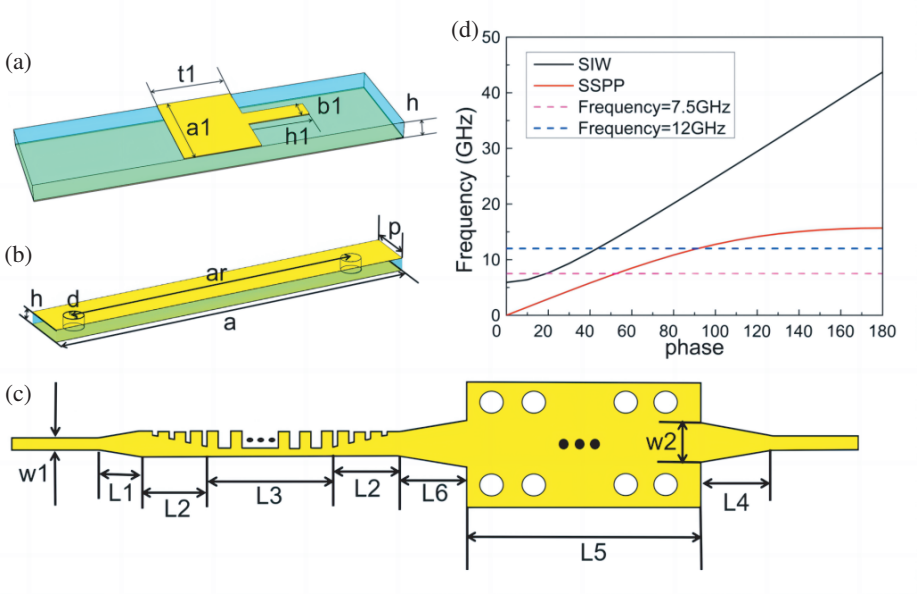

FIGURE 2. The SSPP-SIW hybrid circuit composed of a SIW and an SSPP transmission line. Schematic of the (a) unit cell of the SSPP structure, (b) unit cell of the SIW, (c) the SSPP-SIW hybrid circuit. (d) The dispersion curves of the SIW and the SSPP structures.

nology for dispersion compensation that can be applied to the microwave frequency band. The fast wave in Figure 1(a) represents the wave where high frequency parts propagate with higher speed than the low frequency parts leading to a time delay between the different frequency parts and the broadening of the pulse. The slow wave shows an inverse trend where low frequency parts travel faster than the high frequency parts. By compensating the fast wave dispersion with a corresponding slow wave dispersion, the pulse is recompressed into the original input pulse duration, as shown in Figure 1(b). A transmission line with fast wave characteristics, i.e., a substrate integrated waveguide (SIW), is introduced to compensate the dispersion of traditional SSPP transmission lines. Simulation and experiment results demonstrate that the hybrid circuit allows for minimized group delay variation with the frequency at the receiver within a broad frequency band.

2. DESIGN AND EXPERIMENTAL RESULTS

We propose a hybrid circuit composed of an SSPP transmission line and an SIW connected with a tapered microstrip line, as illustrated in Figure 2 [45]. The unit structures of the SSPP transmission line and SIW are plotted in Figure 2(a) and Figure 2(b), respectively. The commercial material Rogers RO3003 is used as the dielectric substrate with a thickness of $h = 0.508$ mm and a relative permittivity of $\varepsilon r = 3$. The metal layer is made of annealed copper (electric conductivity $\sigma = 5.8e + 007$ S/m) and has a thickness of 0.035 mm. The period, width, strip width, and depth of grooves are $a1 = 3$ mm, $a1 - b1 = 1.8$ mm, $t1 + h1 = 4.4$ mm, and $h1 = 2.2$ mm, respectively. The SSPP transmission line is formed by arranging such units along the x-axis with period a1 on the top surface of the dielectric substrate. We adopt a typical configuration of SIW, whose unit cell is depicted in Figure 2(b). The upper and lower surfaces of the dielectric substrate are metal layers, and the dielectric substrate is separated by two rows of metallic via holes, with a certain distance, $ar = 14.6$ mm. The period of via holes and via diameter are given as $p = 2$ mm and $d = 0.8$ mm, respectively. Figure 2(c) shows the SSPP-SIW hybrid circuit using tapered microstrip lines as transitional structures. The transitional segment structure parameters of the circuit design are obtained through simulation optimization, targeting at the best

TABLE 1. The average slop of group delay spectra for SSPP-SIW hybrid circuits with different lengths of the SIW.

Number of periods	95	99	100	101	105	110
The average group delay slope	-0.0072	-0.0039	-0.0035	-0.0051	-0.0078	-0.0176

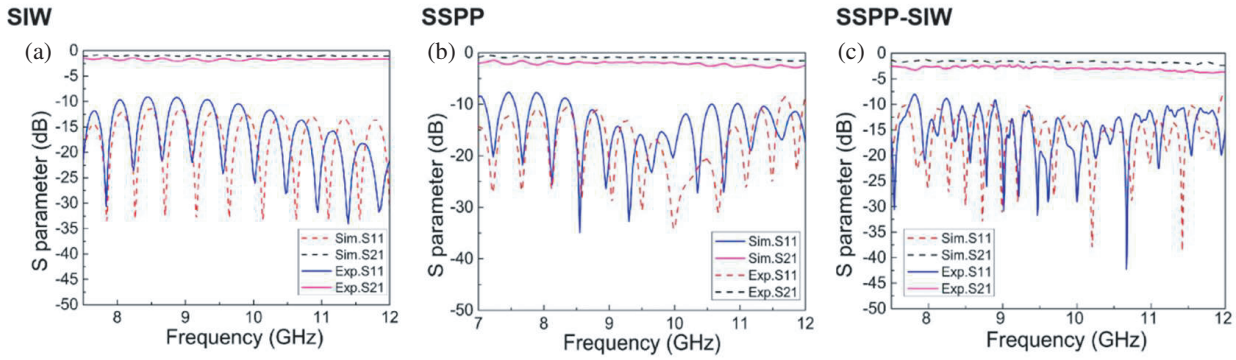

FIGURE 3. The measured and simulated transmission coefficients (S_{21}) and reflection coefficients (S_{11}) of (a) the SIW, (b) the SSPP transmission line, and (c) the SSPP-SIW hybrid circuit.

transmission performance, and the final structural parameters are $w1 = 1.2\,\text{mm}$, $w2 = 8\,\text{mm}$, $L1 = 10\,\text{mm}$, $L2 = 9.45\,\text{mm}$, $L3 = 130.88\,\text{mm}$, $L4 = 15.25\,\text{mm}$, $L5 = 130.4\,\text{mm}$, and $L6 = 12.06\,\text{mm}$.

Here, we employ the eigenmode solver of the commercial software, CST Microwave Studio to calculate the dispersion relations of the SSPP and SIW structures, as shown in Figure 2(d). Within 7.5–12 GHz, we can find that the dispersion curve of SIW shows fast wave characteristics, while the dispersion curve of SSPP shows slow wave characteristics, and their slope change values are almost entirely opposite, satisfying the dispersion compensation requirement as discussed above. In particular, simulated and experimental results show that within the frequency range 7.5–12 GHz, both structures show good transmission performance. As shown in Figure 3, the reflection coefficient S_{11} is basically below $-10\,\text{dB}$, and the signal loss S_{21} is above $-3\,\text{dB}$ for single SIW, SSPP transmission line, as well as the hybrid circuit.

Dispersion effects are visible owing to the fact that the EM wave shows a spectral width which is at least in the same order of magnitude as the modulation bandwidth. Consequently, different wave components will arrive at the receiver with varying time delays leading to pulse broadening or signal distortion. In a modulation system, the dispersion property of a transmission line can be characterized by the group delay (the time delay experienced by a short pulse propagating through the transmission line), calculated by the transmission distance divided by the group velocity (the slope of the dispersion curve) [46–48]. The increased transmission distance can lead to an increased time delay between the different frequency parts, thereby further increasing (or decreasing) the pulse width [49–51]. Thus, as to the hybrid circuit including transmission lines with inverse dispersion trend, there should be an optimized transmission length where minimized group delay dispersion can be achieved. Based on this mechanism, we fix the length of the SSPP transmission line. Here, we consider SSPP-SIW circuits of different lengths and compare their average slopes of group delay spectra in this frequency range for each circuit length, as shown in Table 1. We find that the average slope reaches its minimum value with 100 periods of the SIW structure (corresponding to $L5 = 124.4\,\text{mm}$), indicating that the distortion of signal can be minimized with a hybrid circuit of this length.

We fabricate three transmission lines, i.e., an SSPP transmission line, a SIW, and an SSPP-SIW hybrid circuit, as shown in Figure 4(a), in which the ultrathin copper strips ($t = 0.018\,\text{mm}$) are printed on a Rogers RO3003 dielectric film with thickness of 0.508 mm with PCB technology. To investigate the dispersion compensation performance of this hybrid circuit, three signal probes are positioned at the input end, hybrid circuit connection point, and output end (see Figure 4(a)). We simulate the Ez field of the time-domain waveforms received by the three probes, where the normalized results are plotted in Figure 4(b). We can clearly observe that the pulse is broadened after passing the SSPP transmission line part (probe1-probe2), and compressed back to its original shape after propagating through the SIW segment (probe2-probe3), due to the dispersion compensatory effect.

To further investigate the dispersion performance of the hybrid circuit, we use the vector network analyzer (Agilent N5230C) to measure the group delay of the transmitted signal in the SSPP TL, the SIW, and the SSPP-SIW hybrid circuit. We calculated the group delay of the three types of circuits as a function of the circuit and use the software Origin to preprocess the data to eliminate the impact of noises. In order to intuitively observe the dispersion properties of different circuits, the deviation of each circuit's group delay from its average value within the frequency range of 7.5–12 GHz is calculated with both the simulated and experimental data, as shown in Figure 4(c). We observe that the overall group delay deviation of the hybrid circuit from the average is generally within the range of -0.06 to 0.15, while the SSPP transmission line exhibits an average difference of approximately -0.13 to 0.24, and the SIW demonstrates a mean difference ranging from -0.14 to 0.31. Thus, the group delay of the transmitted signal from the SSPP-SIW hybrid circuit remains relatively stable with varying frequencies as compared with the single SSPP and single SIW cases. Additionally, we calculate the average slope of the group delay spectrum curve with

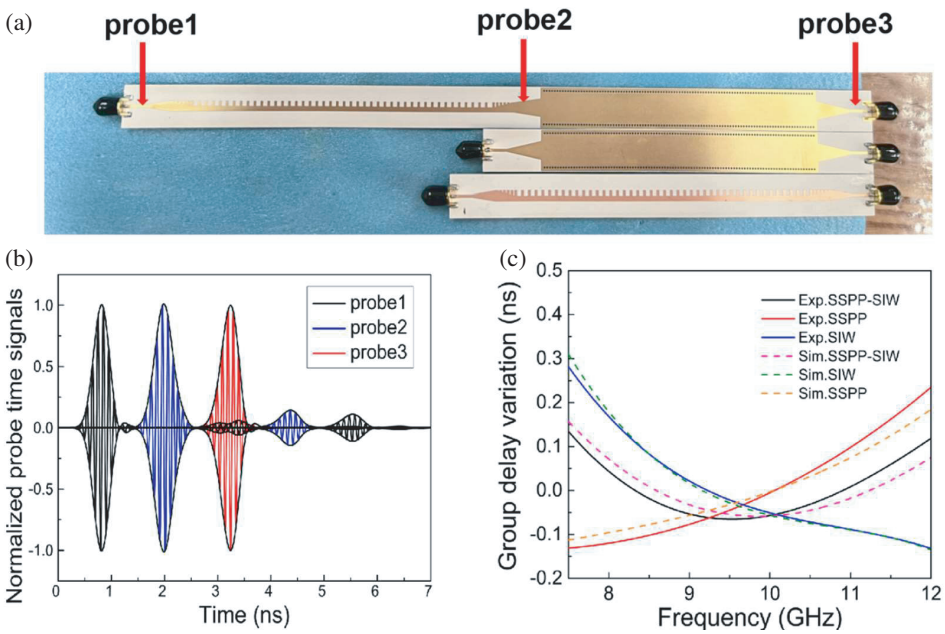

FIGURE 4. (a) Photograph of the fabricated SSPP-SIW hybrid circuit, the SIW, and the SSPP transmission line. (b) The normalized time-domain waveforms of the Ez field received by the three probes. (c) The measured and simulated group delay variation of the transmitted signal from the SSPP transmission line, the SIW, and the SSPP-SIW hybrid circuit.

TABLE 2. The average group delay slope for both experimental and simulated data.

	SSPP TL	SIW	SSPP-SIW hybrid circuit
Simulation results	0.0814	0.0920	−0.0035
Experimental results	0.0661	−0.0989	−0.0182

both experimental and simulated data in three different cases, as presented in Table 2. For the calculation of the results in Table 2, firstly we used the CST software simulation to obtain the S parameter of the SSPP-SIW hybrid circuit at different lengths. The S parameters and phase relations meet the formula:

$$\phi(\omega) = \arctan\left(\frac{\text{lm}}{\text{Re}}\right),$$

in which $\Phi(\omega)$ is the phase under the angular frequency ω, lm the virtual part of S_{21} under the angular frequency ω, and Re the real part of S_{21} under the angular frequency ω.

The group delay and phase follow the following formula:

$$\tau(\omega) = -\frac{d\phi(\omega)}{d\omega} \approx -\frac{\phi_1(\omega) - \phi_2(\omega)}{\omega_1 - \omega_2}.$$

Thus, based on the S parameters obtained by the simulation, we can use the built-in macro in the CST software to directly solve the group delay at different frequency points. Finally, using the Matlab software to calculate the average group delay slope of bybid circuits at different lengths, and we can see that the average slop of group delay spectrum in the SSPP-SIW hybrid circuit approaches 0. The experimental results indicate an impressive improvement of 72.46% for the SSPP transmission line in the stability of the circuit group delay after applying the dispersion compensation approach.

3. CONCLUSION

In this paper, we propose a hybrid circuit approach to realize the dispersion-minimized transmission of the SSPP signals, where the positive dispersion of the SSPP transmission line can be compensated by inserting a piece of transmission line with opposite-dispersion characteristic. Both numerical simulations and experiments are performed to demonstrate the validity of our approaches, where rectification of the signal distortion is observed, and the average slop of the group delay spectrum in the SSPP-SIW hybrid circuit approaches 0. Compared to a single SSPP transmission line, the variation of the group delay with the frequency is minimized, and the group delay stability is increased by 72.46%. Our investigation may further promote the application of SSPP transmission lines in the integrated circuits.

ACKNOWLEDGEMENT

W. Zou and W. Tang contribute equally to this work. This work was supported by the National Natural Science Foundation of China (62271139, U21A20459), the National Key Research and Development Program of China (2022YFA1404903).

REFERENCES

[1] Zhang, J., H.-C. Zhang, X.-X. Gao, L.-P. Zhang, L.-Y. Niu, P.-H. He, and T.-J. Cui, "Integrated spoof plasmonic circuits," *Science Bulletin*, Vol. 64, No. 12, 843–855, 2019.

[2] Ma, H. F., X. Shen, Q. Cheng, W. X. Jiang, and T. J. Cui, "Broadband and high-efficiency conversion from guided waves to spoof surface plasmon polaritons," *Laser & Photonics Reviews*, Vol. 8, No. 1, 146–151, 2014.

[3] Gao, Z., L. Wu, F. Gao, Y. Luo, and B. Zhang, "Spoof plasmonics: From metamaterial concept to topological description," *Advanced Materials*, Vol. 30, No. 31, 1706683, 2018.

[4] Huidobro, P. A., A. I. Fernández-Domínguez, J. B. Pendry, L. Martín-Moreno, and F. J. Garcia-Vidal, *Spoof Surface Plas-*

mon Metamaterials, Cambridge University Press, 2018.

[5] Liu, L. and Z. Li, "Spoof surface plasmons arising from corrugated metal surface to structural dispersion waveguide," *Progress In Electromagnetics Research*, Vol. 173, 93–127, 2022.

[6] Zhang, H. C., Y. Fan, J. Guo, X. Fu, and T. J. Cui, "Second-harmonic generation of spoof surface plasmon polaritons using nonlinear plasmonic metamaterials," *ACS Photonics*, Vol. 3, No. 1, 139–146, 2016.

[7] Cui, W. Y., J. Zhang, X. Gao, and T. J. Cui, "Reconfigurable Mach-Zehnder interferometer for dynamic modulations of spoof surface plasmon polaritons," *Nanophotonics*, Vol. 11, No. 9, 1913–1921, 2022.

[8] Cheng, Y., W. Cao, G. Wang, X. He, F. Lin, and F. Liu, "3D Dirac semimetal supported thermal tunable terahertz hybrid plasmonic waveguides," *Optics Express*, Vol. 31, No. 11, 17 201–17 214, 2023.

[9] Maleki, M. J. and M. Soroosh, "A low-loss subwavelength plasmonic waveguide for surface plasmon polariton transmission in optical circuits," *Optical and Quantum Electronics*, Vol. 55, No. 14, 1266, 2023.

[10] Maleki, M. J., M. Soroosh, and G. Akbarizadeh, "A subwavelength graphene surface plasmon polariton-based decoder," *Diamond and Related Materials*, Vol. 134, 109780, 2023.

[11] Haddadan, F. and M. Soroosh, "Design and simulation of a subwavelength 4-to-2 graphene-based plasmonic priority encoder," *Optics & Laser Technology*, Vol. 157, 108680, 2023.

[12] Mohammadi, M., M. Soroosh, A. Farmani, and S. Ajabi, "Engineered FWHM enhancement in plasmonic nanoresonators for multiplexer/demultiplexer in visible and NIR range," *Optik*, Vol. 274, 170583, 2023.

[13] Chen, Z., P. Cai, Q. Wen, H. Chen, Y. Tang, Z. Yi, K. Wei, G. Li, B. Tang, and Y. Yi, "Graphene multi-frequency broadband and ultra-broadband terahertz absorber based on surface plasmon resonance," *Electronics*, Vol. 12, No. 12, 2655, 2023.

[14] Wu, Y., P. Xie, Q. Ding, Y. Li, L. Yue, H. Zhang, and W. Wang, "Magnetic plasmons in plasmonic nanostructures: An overview," *Journal of Applied Physics*, Vol. 133, No. 3, 030902, 2023.

[15] Ryzhii, V., T. Otsuji, and M. Shur, "Graphene based plasma-wave devices for terahertz applications," *Applied Physics Letters*, Vol. 116, No. 14, 140501, 2020.

[16] Viti, L., J. Hu, D. Coquillat, A. Politano, W. Knap, and M. S. Vitiello, "Efficient terahertz detection in black-phosphorus nanotransistors with selective and controllable plasma-wave, bolometric and thermoelectric response," *Scientific Reports*, Vol. 6, No. 1, 20474, 2016.

[17] Rizza, C., D. Dutta, B. Ghosh, F. Alessandro, C.-N. Kuo, C. S. Lue, L. S. Caputi, A. Bansil, V. Galdi, A. Agarwal, A. Politano, and A. Cupolillo, "Extreme optical anisotropy in the type-II dirac semimetal NiTe2 for applications to nanophotonics," *ACS Applied Nano Materials*, Vol. 5, No. 12, 18 531–18 536, 2022.

[18] Viti, L., D. Coquillat, A. Politano, K. A. Kokh, Z. S. Aliev, M. B. Babanly, O. E. Tereshchenko, W. Knap, E. V. Chulkov, and M. S. Vitiello, "Plasma-wave terahertz detection mediated by topological insulators surface states," *Nano Letters*, Vol. 16, No. 1, 80–87, 2016.

[19] Hu, Z., L. Zhang, A. Chakraborty, G. D'Olimpio, J. Fujii, A. Ge, Y. Zhou, C. Liu, A. Agarwal, I. Vobornik, *et al.*, "Terahertz nonlinear hall rectifiers based on spin-polarized topological electronic states in 1T-$CoTe_2$," *Advanced Materials*, Vol. 35, No. 10, 2209557, 2023.

[20] Guo, C., W. Guo, H. Xu, L. Zhang, G. Chen, G. D'Olimpio, C.-N. Kuo, C. S. Lue, L. Wang, A. Politano, *et al.*, "Ultrasensitive ambient-stable $SnSe_2$-based broadband photodetectors for room-temperature IR/THz energy conversion and imaging," *2D Materials*, Vol. 7, No. 3, 035026, 2020.

[21] Mitrofanov, O., L. Viti, E. Dardanis, M. C. Giordano, D. Ercolani, A. Politano, L. Sorba, and M. S. Vitiello, "Near-field terahertz probes with room-temperature nanodetectors for subwavelength resolution imaging," *Scientific Reports*, Vol. 7, No. 1, 44240, 2017.

[22] Pogna, E. A. A., L. Viti, A. Politano, M. Brambilla, G. Scamarcio, and M. S. Vitiello, "Mapping propagation of collective modes in Bi_2Se_3 and $Bi_2Te_{2.2}Se_{0.8}$ topological insulators by near-field terahertz nanoscopy," *Nature Communications*, Vol. 12, No. 1, 6672, 2021.

[23] Wang, L., L. Han, W. Guo, L. Zhang, C. Yao, Z. Chen, Y. Chen, C. Guo, K. Zhang, C.-N. Kuo, *et al.*, "Hybrid dirac semimetal-based photodetector with efficient low-energy photon harvesting," *Light: Science & Applications*, Vol. 11, No. 1, 53, 2022.

[24] Zhang, L., Z. Chen, K. Zhang, L. Wang, H. Xu, L. Han, W. Guo, Y. Yang, C.-N. Kuo, C. S. Lue, *et al.*, "High-frequency rectifiers based on type-II Dirac fermions," *Nature Communications*, Vol. 12, No. 1, 1584, 2021.

[25] Guo, C., Y. Hu, G. Chen, D. Wei, L. Zhang, Z. Chen, W. Guo, H. Xu, C.-N. Kuo, C. S. Lue, *et al.*, "Anisotropic ultrasensitive $PdTe_2$-based phototransistor for room-temperature long-wavelength detection," *Science Advances*, Vol. 6, No. 36, eabb6500, 2020.

[26] Agarwal, A., M. S. Vitiello, L. Viti, A. Cupolillo, and A. Politano, "Plasmonics with two-dimensional semiconductors: From basic research to technological applications," *Nanoscale*, Vol. 10, No. 19, 8938–8946, 2018.

[27] Tang, W. X., H. C. Zhang, H. F. Ma, W. X. Jiang, and T. J. Cui, "Concept, theory, design, and applications of spoof surface plasmon polaritons at microwave frequencies," *Advanced Optical Materials*, Vol. 7, No. 1, 1800421, 2019.

[28] Cui, T. J., "Microwave metamaterials — From passive to digital and programmable controls of electromagnetic waves," *Journal of Optics*, Vol. 19, No. 8, 084004, 2017.

[29] Cui, T. J., "Microwave metamaterials," *National Science Review*, Vol. 5, No. 2, 134–136, Mar. 2018.

[30] Mahant, K., H. Mewada, A. Patel, A. D. Vala, and J. P. Chaudhari, "Spoof surface plasmon polaritons and half-mode substrate integrated waveguide based compact band-pass filter for radar application," *Progress In Electromagnetics Research M*, Vol. 101, 25–35, 2021.

[31] Shen, X. and T. J. Cui, "Planar plasmonic metamaterial on a thin film with nearly zero thickness," *Applied Physics Letters*, Vol. 102, No. 21, 211909, 2013.

[32] Cao, R.-F. and L. Li, "Modeling and design of CPW spoof surface plasmon polariton with reduced transversal width," *Progress In Electromagnetics Research Letters*, Vol. 113, 1–6, 2023.

[33] Ruan, Z. and M. Qiu, "Slow electromagnetic wave guided in subwavelength region along one-dimensional periodically structured metal surface," *Applied Physics Letters*, Vol. 90, No. 20, 201906, 2007.

[34] Zhang, H. C., L. P. Zhang, J. Lu, C. Shao, P. H. He, W. Y. Cui, Y. F. Huang, and T. J. Cui, "Measurement method for the dispersion curves of a spoof SPP transmission line using a single sample," *IEEE Transactions on Antennas and Propagation*, Vol. 71, No. 2, 1843–1850, 2023.

[35] Zhang, H. C., P. H. He, W. X. Tang, Y. Luo, and T. J. Cui, "Planar spoof SPP transmission lines: Applications in microwave circuits," *IEEE Microwave Magazine*, Vol. 20, No. 11, 73–91,

2019.

[36] Zhang, D., X. Liu, Y. Sun, K. Zhang, Q. Wu, Y. Li, T. Jiang, and S. N. Burokur, "Dispersion engineering of spoof plasmonic metamaterials via interdigital capacitance structures," *Optics Letters*, Vol. 48, No. 6, 1383–1386, 2023.

[37] Dong, G., H. Shi, W. Li, Y. He, A. Zhang, Z. Xu, X. Wei, and S. Xia, "A multi-band spoof surface plasmon polariton coupling metasurface based on dispersion engineering," *Journal of Applied Physics*, Vol. 120, No. 8, 084505, 2016.

[38] Yang, J., J. Wang, X. Zheng, A. Zhang, R. Mittra, and G. A. E. Vandenbosch, "Broadband anomalous refractor based on dispersion engineering of spoof surface plasmon polaritons," *IEEE Transactions on Antennas and Propagation*, Vol. 69, No. 5, 3050–3055, 2021.

[39] Yang, J., J. Wang, M. Feng, Y. Li, X. Wang, X. Zhou, T. Cui, and S. Qu, "Achromatic flat focusing lens based on dispersion engineering of spoof surface plasmon polaritons," *Applied Physics Letters*, Vol. 110, No. 20, 203507, 2017.

[40] Panicker, R. A. and J. M. Kahn, "Algorithms for compensation of multimode fiber dispersion using adaptive optics," *Journal of Lightwave Technology*, Vol. 27, No. 24, 5790–5799, 2009.

[41] Shen, S. and A. M. Weiner, "Complete dispersion compensation for 400-fs pulse transmission over 10-km fiber link using dispersion compensating fiber and spectral phase equalizer," *IEEE Photonics Technology Letters*, Vol. 11, No. 7, 827–829, 1999.

[42] Mao, D., Z. He, Y. Zhang, Y. Du, C. Zeng, L. Yun, Z. Luo, T. Li, Z. Sun, and J. Zhao, "Phase-matching-induced near-chirp-free solitons in normal-dispersion fiber lasers," *Light: Science & Applications*, Vol. 11, No. 1, 25, 2022.

[43] Liu, X., M. Kong, Y. Xu, and X. Wang, "Simulation analysis of the influence of various parameters on output pulse distortion of group velocity control in microring resonator," *Infrared and Laser Engineering*, Vol. 48, No. 9, 918 002–0 918 002, 2019.

[44] Rong, N. Y. and M. Ru, "Investigation on the dispersion characteristics in optical fiber telecommunication," *International Journal of Future Generation Communication and Networking*, Vol. 8, No. 4, 69–80, 2015.

[45] Zhang, Q., H. C. Zhang, H. Wu, and T. J. Cui, "A hybrid circuit for spoof surface plasmons and spatial waveguide modes to reach controllable band-pass filters," *Scientific Reports*, Vol. 5, No. 1, 16531, 2015.

[46] Mikki, S. M. and A. A. Kishky, "Electromagnetic wave propagation in dispersive negative group velocity media," in *2008 IEEE MTT-S International Microwave Symposium Digest*, 205–208, IEEE, Atlanta, GA, USA, 2008.

[47] Ravelo, B., "Investigation on microwave negative group delay circuit," *Electromagnetics*, Vol. 31, No. 8, 537–549, 2011.

[48] Liu, Z., J. Zhang, X. Lei, L. Zhang, K. Wang, and Z. Xu, "A negative group delay rectangular waveguide based on corrugated tantalum nitride slow wave structure," *Microwave and Optical Technology Letters*, Vol. 65, No. 8, 2183–2188, 2023.

[49] Lima, I. T., T. D. S. DeMenezes, V. S. Grigoryan, M. O'sullivan, and C. R. Menyuk, "Nonlinear compensation in optical communications systems with normal dispersion fibers using the nonlinear fourier transform," *Journal of Lightwave Technology*, Vol. 35, No. 23, 5056–5068, 2017.

[50] Ma, T. and M. Skorobogatiy, "Dispersion compensation in the fiber-based terahertz communication links," in *2015 IEEE International Conference on Ubiquitous Wireless Broadband (ICUWB)*, 1–5, IEEE, Montreal, QC, Canada, 2015.

[51] Guerin, M., F. Haddad, W. Rahajandraibe, S. Ngoho, G. Fontgalland, F. Wan, and B. Ravelo, "BI-CMOS design of a*exp (−j *φ0) phase shifter as miniature microwave passive circuit using bandpass NGD resonant circuit," *Progress In Electromagnetics Research B*, Vol. 104, 1–19, 2024.